

Experimental Validation of Applicability of Low-Level Test Methods to Assess the Effectiveness of Shielding From High-Power Electromagnetic Fields

Vladimir Mordachev¹, Eugene Sinkevich¹, Dzmitry Tsyanevka¹, Oleg Mikheev², Konstantin Sakharov², Alexander Sukhov², Vladimir Turkin², Wen-Qing Guo³, Xie Ma³, Hao-Yue Zheng³

¹ EMC R&D Laboratory, Belarusian State University of Informatics and Radioelectronics, Minsk, Belarus, emc@bsuir.by
² All-Russian Scientific Research Institute for Optical and Physical Measurements (VNIIOFI), Moscow, Russia, m12@vniiofi.ru
³ China Electronics Technology Cyber Security Co., Ltd., Chengdu, Taiyuan, China, 18081045600@163.com

Abstract — An experimental validation of the linearity of transfer characteristics for elements of the shielding-type protection of an onboard system against high-power electromagnetic fields is carried out by considering the examples of a metal mesh and a braid of a coaxial cable. The validation technique is based on a comparison of the protection element's amplitude-frequency characteristics obtained at different levels of the electromagnetic test disturbance. The validation is performed for ultra-wideband pulsed disturbance with amplitude up to 50 kV/m, pulse duration of 230 ps, and pulse rise time of 140 ps. The results of the experiments confirmed the applicability of the linear model to the description of the protective properties of shielding elements in the specified range of levels of external disturbance. This fact substantiates the possibility of using the protection element's frequency characteristics measured at low levels of test disturbance to describe the operation of this element in case of protection against disturbances with amplitudes up to 50 kV/m.

Keywords—EMC, electromagnetic shielding, coaxial cables, pulse measurements, electromagnetic transients, IEMI, HPEM

I. INTRODUCTION

In the design and modernization of mobile objects (aircrafts, cars, ships, etc.), an important task is to ensure the protection of their onboard electronic systems from powerful external electromagnetic (EM) fields [1], [2]. To assess the effectiveness of the use of protection elements (shields, gaskets, filters, limiters, etc.), it is necessary to determine the level of system immunity to EM disturbance before and after applying a protective solution. For the purpose of a preliminary assessment of the effectiveness of a single protection element, a standardized test system [3] is used instead of a real system, which simplifies the comparison of protection elements with each other.

Methods of testing the immunity of radio and electronic equipment to radiated electromagnetic disturbances are usually classified into high-level (the level of test field, as a rule, exceeds 100 V/m) and low-level [4], [5]. The advantage of the low-level methods is their simplicity and low cost of experiments as compared to high-level tests. The disadvantage of the low-level methods is that they do not take into account

non-linear effects which may occur in the test object under the influence of powerful electromagnetic fields [4].

At high levels of the field, the nonlinear effects can be observed even in objects that are traditionally regarded as linear, for example, in the elements of passive protection of an onboard system from external electromagnetic disturbances. In particular, a diode effect (nonlinearity of the surface properties of materials due to corrosion, moisture, organic contamination) and insulation breakdown may occur in the shields [4].

To confirm the applicability of the results of low-level tests to the description of the test object operation at high levels of disturbance, it is necessary to prove the absence of nonlinear effects in this object at high levels of disturbance.

Ultra-wideband EM pulses (UWB EMPs) can be considered as a relatively new type of powerful EM disturbances [2], [5]. The onboard electronic equipment of mobile objects can be efficiently damaged by UWB EMPs [6]. The results of measuring the properties of radio absorbing materials by irradiating them with UWB EMPs are given in [7]. The penetration of powerful UWB EMPs into fortified underground objects was investigated in [8].

The objective of this work is the experimental investigation of the possibility of using a linear model for describing the protective properties of the shielding elements of a system in case of exposure of these elements to UWB EMPs with amplitude up to 50 kV/m. The results of the study will confirm or disprove the applicability of low-level test methods [3], [4], [9], [10] to determine the performance characteristics of shielding protective elements.

It was decided to perform the study by consideration of the following typical widely-used shielding-type protection elements as examples: 1) a metal mesh on the aperture and 2) a braided shield (braid) of a coaxial cable.

II. TECHNIQUE FOR EXPERIMENTAL VALIDATION OF LINEARITY OF SHIELDS

In the framework of linear models of technical means of protection against electromagnetic disturbances, transfer

functions are introduced to describe the protection elements [3], [11]. Experimental proof of the linearity of the shielding protective element (metal mesh, gasket, etc.) may be confirmation of the independence of the amplitude-frequency characteristic (AFC, i.e., the absolute value of the transfer function) of this element from the amplitude-time characteristics of the exciting electromagnetic radiation.

Analysis of the shielding properties of the protective element in the form of a metal mesh is reasonable to carry out by installing this mesh on the aperture located in the door of the shielded box. Then the AFC of the mesh is determined by the ratio (see [3], [12], [13]):

$$K_{mesh}(f) = |E_{closed}(f)| / |E_{open}(f)|, \quad (1)$$

where $E_{open}(f) = \text{FFT}\{E_{open}(t)\}$ – is the response spectrum, which is determined as the direct Fourier transform $\text{FFT}\{\}$ from the time-domain realization of pulse $E_{open}(t)$, registered by the oscilloscope when the door of shielded cabin is open (oscilloscope is connected to the field sensor mounted inside the box);

$E_{closed}(f) = \text{FFT}\{E_{closed}(t)\}$ – is the response spectrum, which is determined as the direct Fourier transform from the time-domain realization of pulse $E_{closed}(t)$ obtained when the door of shielded box is closed.

AFC of coaxial cable braid is as follows:

$$K_{coaxial}(f) = |U_{c-shield}(f)| / |E_0(f)|, \quad (2)$$

where $U_{c-shield}(f) = \text{FFT}\{U_{c-shield}(t)\}$ – is the spectrum of voltage between the central wire of coaxial cable and its grounded shield (braid), which is determined as the direct Fourier transform from the time-domain realization of the voltage $U_{c-shield}(t)$ registered by the oscilloscope. The oscilloscope is connected to the one end of the cable, and the second end of the cable is connected to the matched load of resistance 50 Ohm. Part of cable irradiated by the pulsed EM field is placed inside the anechoic chamber;

$E_0(f) = \text{FFT}\{E_0(t)\}$ – is the spectrum of the electric field strength pulse disturbing the coaxial cable. This spectrum is determined as the direct Fourier transform from the time-domain realization of the pulse $E_0(t)$, registered by the oscilloscope. The oscilloscope is connected to the field sensor placed instead the coaxial cable in the point that were the geometrical center of irradiated part of the cable.

If values of AFCs (1) – (2) obtained as the result of experiments for the pulses with the different amplitudes will be equal to each other within the error estimates, it proves the linearity of the corresponding protective solution up to the maximum achievable value of the pulse amplitude in the experiment.

Experimental proof of the linearity of objects under test based on an analysis of their responses to a pulse disturbance is possible only in a certain frequency range, i.e., in the effective band of frequencies of the emitted pulse. This band is defined as the frequency range, which contains 90 % of the pulse energy (5 % of the pulse energy is concentrated at the frequencies that are less than the lower limit of this range, and 5 % of the pulse energy is concentrated at the frequencies above the upper limit of this range). Outside the effective band of frequencies, the EMP energy is low, and therefore the random measurement error of AFC (due to the influence of internal noise of measurement equipment and external interference) increases rapidly [4]. Therefore, the comparison of AFC obtained using different sources of EMP is correct only in the intersection of the effective frequency bands of the corresponding EMPs.

III. DESCRIPTION OF TEST FACILITY

A. Equipment Used in Measurements

The following equipment is used during the tests.

1. The test complex of pulsed electromagnetic fields, which includes Pulsed Voltage Generators (PVGs) (PVG5-1000 and PVG50-1000), antenna-feeder device that contains a radiator (an array of 4 TEM-horns with a length of 0.5 m and an aperture of 0.5 x 0.5 m) and high-voltage feeders for connecting the PVGs to the radiator. The amplitude of the voltage pulse at the generator output is 5 kV for PVG5-1000 and 50 kV for PVG50-1000; generators provide the formation of both single pulses and burst with a pulse repetition rate in a burst of up to 1000 Hz.

2. Measuring sensor of the pulsed electric field intensity (E-field Strip Line Sensor (SLS), hereinafter – E-field sensor) equipped with a 50-Ohm coaxial transmission line [14]. Sensor conversion factor $K_{trSLS} = 5.49 \cdot 10^{-4}$ V/(V/m), relative error is ± 3.7 %, transient response rise time $T_{trSLS} = 50$ ps, clear time is $T_{cr} = 4.4$ ns, relative error of time interval measurements is ± 3.5 %.

3. Digital storage oscilloscope Tektronix DPO 71604 (bandwidth is 16 GHz; rise time $T_{trOsc} = 22.5$ ps; input impedance is 50 Ohm). The effective number of bits of the oscilloscope is 5.5; therefore, the quantization error does not exceed 1.1 %.

4. High-frequency high-voltage attenuators. Attenuation (transformation) factors are: $K_{1Aten} = 10.11$, $K_{2Aten} = 10.0$. Expanded uncertainty of transformation factor is 1.6 % ($P = 0.95$, $k = 2$). The rise time is $T_{trAten} = 20$ ps. Maximum allowable amplitude of measured values of voltage pulses (with a pulse duration of up to 100 ns and a frequency of pulses in the burst of 1 kHz) is 4000 V.

5. The shielded room to arrange the measuring equipment and to accommodate the personnel responsible for operation with it. The shielding effectiveness is at least 30 dB in the

frequency range from 0.1 to 1.0 GHz, the attenuation coefficient of network interference is at least 30 dB.

6. A mobile shielded box in the form of a rectangular parallelepiped with dimensions of $0.55 \times 0.65 \times 0.85$ m is used as the shielded box under test. One wall of the box is a door made of aluminum sheet 3 mm thick. There is a 0.3×0.3 m aperture in the door; the aperture is covered with a wire mesh with 2.5×2.5 mm cells. The material of the side walls is a wire mesh made of aluminum with a thickness of 1.5 mm, the mesh cell is 2 mm.

7. The RF coaxial cable of RK 50-7-11 type is used as a coaxial cable under test. Insulator is a low density polyethylene with a diameter of (7.25 ± 0.15) mm, the inner conductor is twist from 7 copper wires with a nominal diameter of 2.28 mm, outer conductor is braid from copper wire (nominal diameter of 0.15 mm, weaving density is 88-92 %, braid angle is $50-60^\circ$). Characteristic impedance is (50 ± 2) Ohms, attenuation coefficient at 3 GHz frequency is 1.2 dB/m.

B. Experimental Setup for Testing the Shield in Form of Metal Mesh

Block diagram with the connection of the equipment when testing a shielded box with a metal mesh is shown in Figure 1. The E-field SLS sensor is installed inside the box along the direction of the radiation axis of the antenna. The distance from the mesh under test to the marker point of the sensor is (5.0 ± 1.0) cm. The distance between the marker points of the radiating system and the sensor is (1.65 ± 0.05) m, the polarization of radiation is vertical.

In order to test the linearity of the shielding properties of the metal mesh covering the aperture in the door of the shielded box, two oscillograms of the voltage at the sensor output were obtained at a constant relative position of the sensor and antenna. The first oscillogram corresponds to the case when the boxes' door is open and the second one – to the case of closed door of the box. Generators of high voltage pulses PVG5-1000 and PVG50-1000 were used as the source of disturbance.

C. Experimental Setup for Testing the Shield in Form of Coaxial Cable Braid

Block diagram with the connection of the equipment in the case under consideration is presented in Figure 2.

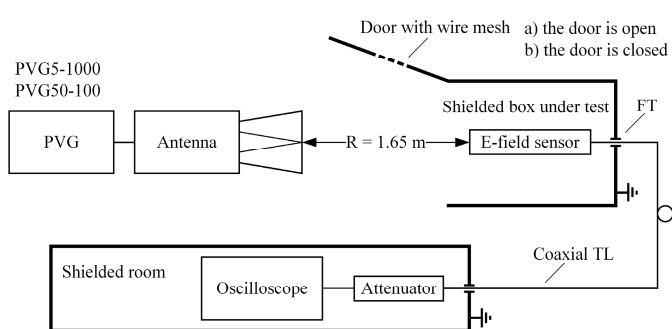


Fig. 1. Experimental setup for analysis of shielding properties of metal wire mesh: a) the door is open; b) the door is closed. Notations: FT is feedthrough, TL is transmission line, PVG is pulsed voltage generator

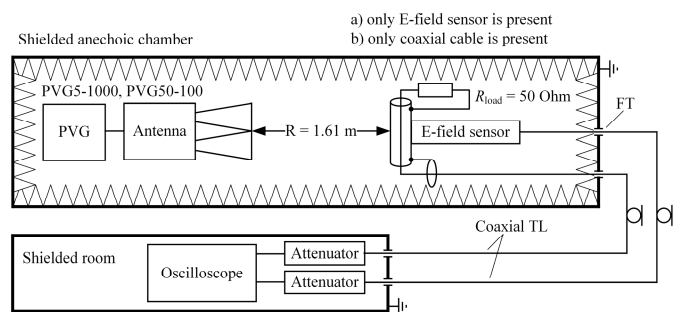


Fig. 2. Experimental setup for testing the braid of coaxial cable. Notations are the same as in Figure 1.

The following measurements were carried out in order to check the linearity of the shielding properties of the coaxial cable braid.

1. For determination of the amplitude-time parameters of the disturbing EMP, the field sensor is installed in the anechoic shielded chamber at a point that will correspond to the geometric center of the irradiated section of the coaxial cable (the cable will be irradiated instead of the sensor during the measurement No. 2, see next paragraph).

2. Voltage induced on the central wire of the coaxial cable is determined when the cable is placed in the pulsed field. The horizontal section of the coaxial cable is irradiated, the length of the irradiated section is 0.6 m. A matched coaxial load is connected to one end of the cable, the cable braid is grounded to the shield of the anechoic shielded camera. The other end of the cable is connected to the input of the oscilloscope by the use of corresponding attenuator.

IV. RESULTS OF EXPERIMENT AND THEIR ANALYSIS

A. Analysis of Reference Pulses

The initial stage of the analysis is the determination of the characteristics of the test pulses emitted by the antenna-feeder device of the test complex. These pulses are called reference pulses. The effective frequency band used for further analysis is determined for reference pulses. Waveforms of pulses at the output of the E-field SL sensor, obtained when the antenna-feeder device is excited by the PVG5-1000 generator, are shown in Figure 3.

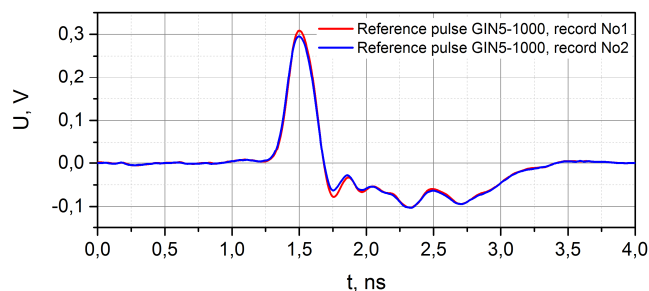


Fig. 3. Oscillogram of the voltage of the reference pulse obtained when the generator PVG5-1000 is connected to the antenna-feeder device. Two series of experiments with the same conditions were carried out: record No1 (red line) and record No2 (blue line) are the results. A rectangular time window of 3.7 ns width was used

The values of the parameters of the reference pulse at the point of E-field sensor location are obtained on the basis of the digitized voltage waveform by the following formulas:

$$E_{\max} = \frac{U_{\max}}{K_{trSLS}} \cdot K_1 A_{ten}, \quad (3)$$

$$T_{E\ rise} = \sqrt{T_{U\ rise}^2 - T_{trSLS}^2 - T_{trOsc}^2 - N \cdot T_{trAten}^2},$$

where U_{\max} is the amplitude of the voltage pulse at the E-field sensor output; $T_{U\ rise}$ is the rise time of the voltage pulse. The results are as follows: electric field amplitude is $E_{5ref} = 5.73 \text{ kV/m} \pm 7\%$; rise time of the field pulse (defined by levels of 0.1 and 0.9 from amplitude) is $T_{5\ rise} = 129 \text{ ps} \pm 4\%$; full width at half maximum (FWHM) is $T_{5\ pulse} = 216 \text{ ps} \pm 4\%$ (FWHM of the field pulse is equal to the FWHM of the voltage at the sensor output).

Normalized integral distribution of pulse energy fluence

$$W_{NORM}(f) = \frac{1}{S} \int_{f_{low}}^{f_{high}} |E_0(f)|^2 df, \quad s = \int_0^{\infty} |E_0(f)|^2 df \quad (4)$$

defines the effective band of frequencies of the pulsed field when connecting PVG5-1000: $\Delta f_{5eff} \equiv [f_{low}, f_{high}] = [0.18, 2.42] \text{ GHz}$ (see Fig. 4).

A similar analysis was carried out for the reference pulse emitted by the test complex using the generator PVG50-1000 (see Figure 5). The following characteristics of the field pulse at the observation point were obtained: the amplitude is $E_{50ref} = 52.57 \text{ kV/m} \pm 7\%$, the rise time is $T_{50\ rise} = 145 \text{ ps} \pm 4\%$, FWHM is $T_{50\ pulse} = 230 \text{ ps} \pm 4\%$, the effective band of frequencies is $\Delta f_{50eff} = [0.17, 2.31] \text{ GHz}$.

Therefore, a comparison of AFCs should be performed in the frequency range $[f_{min}, f_{max}] = [0.18, 2.31] \text{ GHz}$ (see Section II).

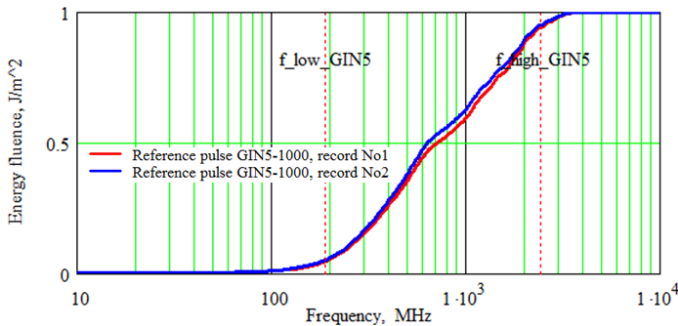


Fig. 4. Normalized integral distribution of energy fluence of the reference pulse obtained when PVG5-1000 is connected to the antenna-feeder device. The boundaries of the effective band of frequencies, which is determined at 90% of the energy (see Section II), are indicated by red dashed lines.

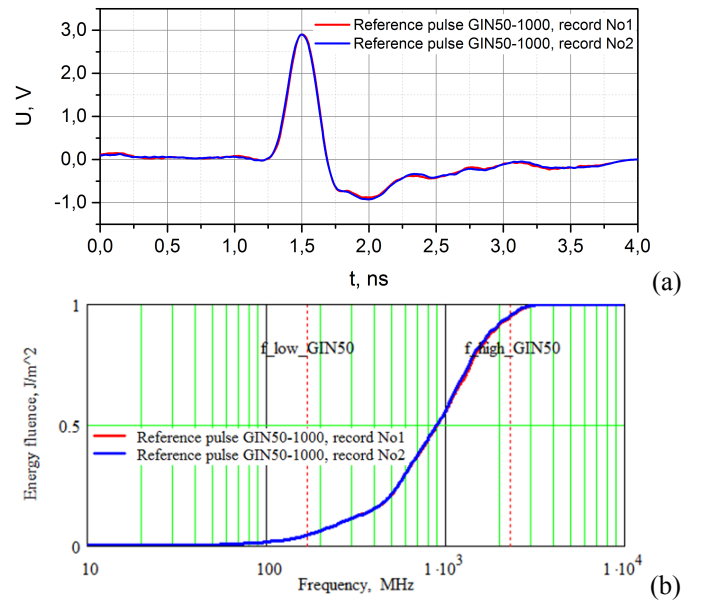


Fig. 5. Characteristics of the reference pulse obtained when PVG50-1000 is connected to the antenna-feeder device: (a) Oscillogram of the voltage at E-field sensor output (the rectangular time window of 3.7 ns width was used), (b) Normalized integral distribution of energy fluence

B. Analysis of AFC of the Shield in Form of Metal Mesh

The oscillograms of the voltage at the output of the E-field SLS, obtained for the both cases (open and closed door of the box), are shown in Figure 6. The corresponding AFCs of the metal mesh $K_5(f)$ and $K_{50}(f)$ calculated by the formula (1) are shown in Figure 7. The ratio of these AFC $R(f) = K_{50}(f)/K_5(f)$ is shown in Figure 8.

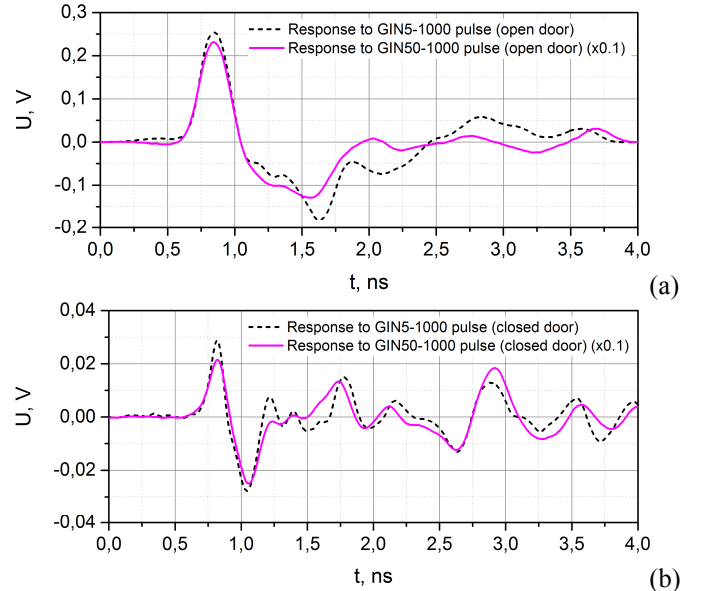


Fig. 6. Time-domain realizations of the voltage at the input of the oscilloscope. The E-field sensor is placed in the shielded box with the opened door (a) and with the closed door (b). The black dashed line is the response to the PVG5-1000 generator pulse, the purple solid line is the 10-times-reduced response to PVG50-1000 pulse. The width of the time window is (a) 3.7 ns, (b) 3.9 ns

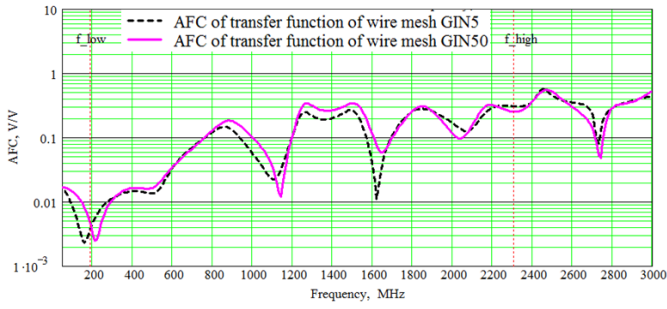


Fig. 7. AFCs of the metal mesh: $K_5(f)$ is obtained by the use of PVG5-1000 (black dashed line), and $K_{50}(f)$ is obtained by the use of PVG50-1000 (purple solid line). The boundaries of the frequency band in which the comparison of these AFCs is correct are indicated by red dotted lines

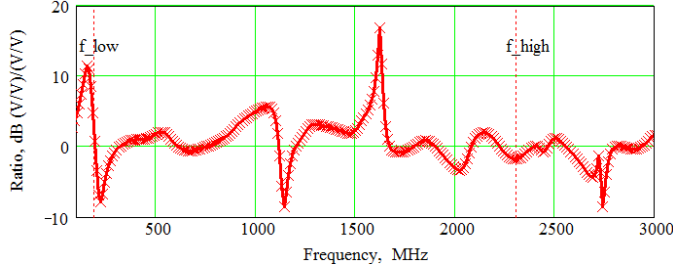


Fig. 8. Ratio of the metal mesh AFCs presented in Figure 7

To reduce the effect of random errors of the measurements, we calculate the average value of the ratio of AFCs

$$R_{av,dB} = \frac{1}{f_{max} - f_{min}} \int_{f_{min}}^{f_{max}} 20 \lg\{R(f)\} df \quad (5)$$

in the frequency band of analysis $[f_{min}, f_{max}] = [0.18, 2.31]$ GHz (see Subsection IV.A). For the metal mesh, it is equal to $R_{av,mesh,dB} = 1.02$ dB (see Figure 8).

The presented results show that the AFC of the metal mesh, obtained using the PVG5-1000 and PVG50-1000 (see Figure 7), can be considered identical within the measurement error.

C. Analysis of AFC of the Shield in Form of Coaxial Cable Braid

Oscillograms of voltages obtained when coaxial cable RK50-7-11 is connected to the input of the oscilloscope are shown in Figure 9. The corresponding AFCs of the coaxial cable braid $K_5(f)$ and $K_{50}(f)$ calculated by formula (2) are shown in Figure 10. The ratio of these AFCs is shown in Figure 11. The average value of the ratio of AFCs calculated by formula (5) is $R_{av,coaxial,dB} = 1.96$ dB.

Note that the positive value of index (5) indicates the presence of a systematic measurement error. An indicator of the presence of non-linear effects would be a significant negative value of $R_{av,dB}$, which means that inequality $K_{50}(f) < K_5(f)$ is satisfied for most of the analysis frequency band.

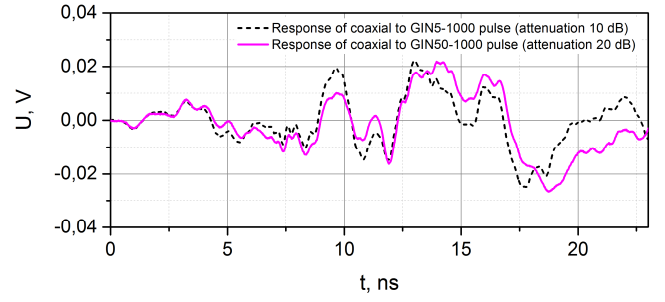


Fig. 9. Time-domain realizations of the voltage at the input of the oscilloscope. The black dashed line is the response of the coaxial cable to the PVG5-1000 generator pulse, the purple solid line is the 10-times-reduced response of the same cable to the GIN50-1000 pulse. The width of the time window is 3.3 ns

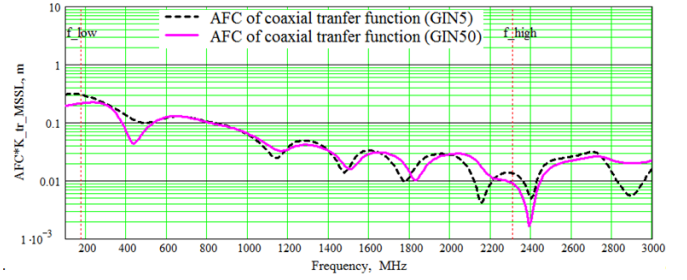


Fig. 10. AFCs of the coaxial cable braid: $K_5(f)$ is obtained by the use of PVG5-1000 (black dashed line), and $K_{50}(f)$ is obtained by the use of PVG50-1000 (purple solid line). The boundaries of the frequency band in which the comparison of these AFCs is correct are indicated by red dotted lines

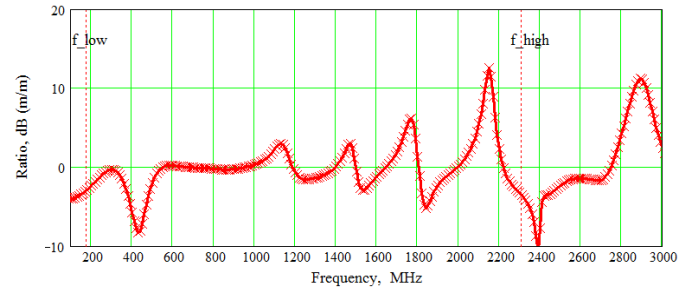


Fig. 11. Ratio of the cable braid AFCs presented in Figure 10

The results show that the AFC of the coaxial cable braid, obtained using PVG5-1000 and PVG50-1000 (see Figure 10), can be considered equal within the limits of measurement error.

D. Peculiarities of Processing of Measurement Results

In equations (1) – (5), continuous functions of the form $E(t)$ are used for simplicity. In reality, one operated with sequences of the form E_n , where n is the sample number ($n = 0 \dots N - 1$) and N is the total number of samples. The sampling period $\Delta t = 5$ ps.

Since the measuring sensor has a limited time window $T_{ct} = 4.4$ ns (see subsection III.A), the readings that do not fall into this window were discarded.

Before performing the Fourier transform, signals were multiplied by a smoothing trapezoidal window w_n in order to minimize the Gibbs effect:

$$w_n = \begin{cases} 0.5 \cdot \left(1 - \cos\left(\frac{\pi \cdot n}{h+1}\right)\right), & 0 \leq n \leq h; \\ 1, & h < n < N-h; \\ 0.5 \cdot \left(1 - \cos\left(\frac{\pi \cdot (N-n)}{h+1}\right)\right), & N-h \leq n < N, \end{cases} \quad (6)$$

where h is the rise time of the window ($h = (N-2)/10$).

The shape of the window is taken to be trapezoidal because the main lobe of the spectrum is very narrow for such window.

To obtain the required frequency discretization step, the recorded sequences were padded with zero samples in time domain. The frequency step was taken to be $\Delta f = 10$ MHz. Therefore the total number of samples together with zero samples was $N = (\Delta t \cdot \Delta f)^{-1} = 2 \cdot 10^4$.

During the calculation of amplitude spectrum AS_n , the correction for the equivalent noise bandwidth (ENBW) of the trapezoidal window was made:

$$AS_n = |S_n| \cdot 2N / \sqrt{ENBW}, \quad ENBW = \sum_{n=0}^{N-1} w_n, \quad (7)$$

where S_n is the result of the Fast Fourier Transform of weighted sequence $w_n \cdot E_n$. Afterwards, the sequences of the form AS_n were used in calculations of frequency responses (1), (2) and energy distribution (4).

V. CONCLUSION

The impact of UWB EMPs on the shielding-type protection elements (a metal mesh and a coaxial cable braid) is studied experimentally. For each of the protection elements considered as examples, it is established that AFCs obtained at different amplitudes of EMPs can be regarded as identical in the effective band of frequencies (from 180 MHz to 2.31 GHz) of the reference pulse.

The results of the experiments confirmed that the linearity of the shielding properties (i.e., their independence from the amplitude of the disturbance) is specific to both objects under test up to the pulse amplitude of 50 kV/m. This fact substantiates the possibility of using the protection element's AFCs measured at low levels of test disturbances to describe the operation of this element in case of protection against disturbances with amplitudes up to 50 kV/m.

The technique used in the experiments can be applied to measure the frequency characteristics of the shielding effectiveness of various objects in a wide range of frequencies. As compared with traditional measurement methods that use continuous-wave test excitation, the main advantage of the measurements based on UWB EMP excitation is their high speed [15].

For pulsed excitation of the test object, the instantaneous power of the incident radiation achieves large values, but its total energy and average power are small due to short duration of the pulses. For the pulses considered in this paper, the

energy flux density is about 10 mJ/m²/pulse. The time interval between the neighboring pulses (1 ms and more, see subsection III.A) significantly exceeds the relaxation time of the considered test objects, therefore the effect of each pulse in a burst can be considered equal to the effect of the single pulse.

REFERENCES

- [1] MIL-STD-464C. Electromagnetic Environmental Effects Requirements for Systems. U.S. Government Printing, Washington, 2010.
- [2] IEC TR 61000-1-5 International Standard. Electromagnetic Compatibility (EMC) – Part 1-5. General High power electromagnetic (HPEM) effects on civil systems, First edition, 2004-11.
- [3] IEC 61000-4-23, International Standard. Electromagnetic Compatibility (EMC) - Part 4-23: Testing and measurement techniques – Test methods for protective devices for HEMP and other radiated disturbance”, First edition, 2000-10.
- [4] IEC TS 61000-5-9. International Standard. Electromagnetic compatibility (EMC) – Part 5-9: Installation and mitigation guidelines – System-level susceptibility assessments for HEMP and HPEM. Edition 1.0, 2009-07.
- [5] IEC 61000-2-13 International Standard. Electromagnetic Compatibility (EMC) – Part 2-13. Environment – High-power electromagnetic (HPEM) environments – Radiated and conducted. Edition 1.0, 2005-03.
- [6] Sakharov K.Y. et al. Study of UWB Electromagnetic Pulse Impact on Commercial Unmanned Aerial Vehicle // Proc. of 2018 Intern. Symp. on Electromagnetic Compatibility (EMC EUROPE), pp. 40-43.
- [7] Turkin V.A. et al. Measurement of the Reflectivity of Radiation Absorbent Materials by Pulsed Spectroscopy // Measurement Techniques, 2018, Vol. 60, No. 12, pp. 1252-1255.
- [8] Tesche F.M. et al. Coupling and Interaction of High-Power Electromagnetic (HPEM) Radiation With Underground Facilities // International Union of Radio Science. XXIX General Assembly, 7-16 August 2008, Chicago, USA.
- [9] A. Wraight, F. Sabath, A. Brenner, and C. C. Jones, “EMP qualification of a modern fighter aircraft,” in Proc. IEEE Antennas Propag. Soc. Int. Symp. and USNC/URSI Nat. Radio Science Meeting and AMEREM Meeting, Jul.2006, p. 187.
- [10] IEC 61000-4-21 International Standard. Electromagnetic Compatibility (EMC) – Part 4-12. Testing and measurement techniques – Reverberation chamber test methods. Edition 2.0, 2011-01.
- [11] Paul C.R., Introduction to Electromagnetic Compatibility, 2nd ed., Wiley, Hoboken, NJ, 2006, 983 p.
- [12] IEEE Std 299-2006, IEEE Standard Method for Measuring the Effectiveness of Electromagnetic Shielding Enclosures, IEEE Electromagnetic Compatibility Society, IEEE, 3 Park Avenue, New York, NY 10016-5997, USA, 28 February 2007.
- [13] Marvin A.C. et al. A Proposed New Definition and Measurement of the Shielding Effect of Equipment Enclosures // IEEE Trans. on EMC Vol. 47 No. 3, 2005, pp. 589-601.
- [14] Dobrotvorsky, M.I. et al. “Measuring Instruments of Powerful UWB EMP Parameters”, Proc. Of 3rd Int. Conf. on Ultrawideband and Ultrashort Impulse Signals UWBUSIS-2006, Sevastopol, Sept.2006, pp. 373-375
- [15] Sakharov K.Y. et al. Methods and Means of Probing Radio-Absorbing Materials with Ultrashort Electromagnetic Pulses // Measurement Techniques, 2016, Vol. 58, No. 11, pp. 1269-1273.